On the Impact of Phase Shifting Designs on IRS-NOMA

Zhiguo Ding, *Fellow, IEEE*, Robert Schober, *Fellow, IEEE*, and H. Vincent Poor, *Fellow, IEEE*

***Abstract*—In this letter, the impact of two phase shifting designs, namely random phase shifting and coherent phase shifting, on the performance of intelligent reflecting surface (IRS) assisted non-orthogonal multiple access (NOMA) is studied. Analytical results are developed to show that the two designs achieve different tradeoffs between reliability and complexity. Simulation results are provided to compare IRS-NOMA to conventional relaying and IRS assisted orthogonal multiple access, and also to verify the accuracy of the obtained analytical results.**

I. Introduction

Recently, intelligent reflecting surfaces (IRS) have received significant attention, due to their ability to intelligently reconfigure wireless communication environments for better reception reliability at a low cost [1]–[4]. Similar to finite-resolution analogue-beamforming (FRAB), each reflecting element on the IRS changes the phase of the reflected signal only, without modifying its amplitude [5]. As a new energy and spectrally efficient technique, IRS have been recently shown compatible with various advanced communication techniques, including millimeter-wave communications, unmanned aerial vehicle networks, physical layer security, simultaneous wireless information and power transfer [6]–[8].

In this letter, we investigate how the phase shifting design affects the performance of IRS assisted non-orthogonal multiple access (NOMA). Two types of phase shifting designs are considered. The first one is coherent phase shifting, where the phase shift of each reflecting element is matched with the phases of its incoming and outgoing fading channels. Despite its superior performance, coherent phase shifting might not be applicable in practice because of the finite resolution of practical IRS phase shifters and the excessive system overhead caused by acquiring channel state information (CSI) at the source. This motivates the second design employing random phase shifting, where the scheme developed in [9] can be viewed as a special case. The central limit theorem (CLT) is shown to be an accurate approximation tool for analyzing the performance of the random phase shifting scheme. In contrast, for the coherent phase shifting scheme, the approximation obtained with the CLT is accurate at low signal-to-noise ratio (SNR) only. This motivates the development of an upper bound on the outage performance, which is shown to be more accurate than the CLT-based result in the high SNR regime.

II. System Model

Consider a cooperative communication scenario with one source and two users, denoted by U_1 and U_2, respectively. We assume that a direct link is not available between the source and U_1 due to severe blockage. Three cooperative communication strategies are described in the following subsections, respectively.

Z. Ding and H. V. Poor are with the Department of Electrical Engineering, Princeton University, Princeton, NJ 08544, USA. Z. Ding is also with the School of Electrical and Electronic Engineering, the University of Manchester, Manchester, UK (email: zhiguo.ding@manchester.ac.uk, poor@princeton.edu). R. Schober is with the Institute for Digital Communications, Friedrich-Alexander-University Erlangen-Nurnberg (FAU), Germany (email: robert.schober@fau.de).

1) IRS-NOMA: IRS-NOMA ensures that the two users are simultaneously served. In particular, the source broadcasts the superimposed message, $c_1 s_1 + c_2 s_2$, where s_i denotes the unit-power signal for U_i, c_i denotes the power allocation coefficient and we assume that $c_1 \geq c_2$ and $c_1^2 + c_2^2 = 1$.

The signals received by U_1 and U_2 are given by

$$y_1 = \frac{\mathbf{g}_1^H \mathbf{\Theta} \mathbf{g}_0}{\sqrt{d_r^\alpha d_{r1}^\alpha}} \sqrt{P_s} \left(c_1 s_1 + c_2 s_2 \right) + w_1, \tag{1}$$

and

$$y_2 = \left(\frac{h_2}{\sqrt{d_2^\alpha}} + \frac{\mathbf{g}_2^H \mathbf{\Theta} \mathbf{g}_0}{\sqrt{d_r^\alpha d_{r2}^\alpha}} \right) \sqrt{P_s} \left(c_1 s_1 + c_2 s_2 \right) + w_2, \tag{2}$$

where P_s denotes the power used by the source, $\mathbf{\Theta}$ denotes the $N \times N$ diagonal phase shifting matrix with its N main diagonal elements representing the reflecting elements of the IRS, $\mathbf{g}_i$ denotes the fading vector between the IRS and U_i, $\mathbf{g}_0$ denotes the fading vector between the source and the IRS, h_2 and d_2 denote the Rayleigh fading gain and the distance from the source to U_2, respectively, d_r and d_{ri} denote the distances from the IRS to the source and U_i, respectively, w_i denotes the noise at U_i, and α denotes the path loss exponent. We assume that the noise power is normalized and all fading gains are complex Gaussian distributed with zero mean and unit variance, i.e., $\mathcal{CN}(0,1)$.

U_1 treats s_2 as noise when decoding its own signal, s_1, which means that the outage probability achieved by IRS-NOMA is given by

$$\mathrm{P}_1^{\mathrm{NOMA}} = \mathrm{P}\left(\log\left(1 + \frac{P_s c_1^2 \frac{\left| \mathbf{g}_1^H \mathbf{\Theta} \mathbf{g}_0 \right|^2}{d_r^\alpha d_{r1}^\alpha}}{P_s c_2^2 \frac{\left| \mathbf{g}_1^H \mathbf{\Theta} \mathbf{g}_0 \right|^2}{d_r^\alpha d_{r1}^\alpha} + 1} \right) < R_1 \right), \tag{3}$$

where R_i denotes U_i's target data rate and $\mathrm{P}(E)$ denotes the probability of event E. We note that the reflecting path in (2) can be insignificantly weaker than the direct link. For example, for a case with $d_2 = d_r$, $d_{r2} = 10$ m and $\alpha = 4$, the path loss of the reflecting path is 10^4 times larger than that of the direct link. For such scenarios, U_2's outage probability is similar to that in conventional NOMA without IRS.

2) Conventional Relaying: A straightforward benchmarking scheme is cooperative OMA transmission without IRS, which involves two phases. The first phase needs to be further divided into two time slots. During the first time slot, the source sends s_1 to U_2, and during the second time slot, U_2 forwards s_1 to U_1, if it can decode s_1. Otherwise, U_2 keeps silent. During the second phase, the source serves U_2 directly. Therefore, the outage probabilities for U_i are given by

$$\mathrm{P}_1^{\mathrm{OMA}} = \mathrm{P}\left(E_1 \right) + \mathrm{P}\left(\frac{1}{4} \log\left(1 + P_r \frac{|h_{12}|^2}{d_{12}^\alpha} \right) < R_1, E_1^c \right),$$

and $\mathrm{P}_2^{\mathrm{OMA}} = \mathrm{P}\left(\frac{1}{2}\log\left(1+P_2\frac{|h_2|^2}{d_2^\alpha}\right) < R_2\right)$, where $E_1 \triangleq \left\{\frac{1}{4}\log\left(1+P_1\frac{|h_2|^2}{d_2^\alpha}\right) \le R_1\right\}$, respectively, E_1^c denotes the complementary event of E_1, h_{12} and d_{12} denote the fading gain and the distance between the two users, respectively, P_i denotes the source's transmit power for U_i's signal, and P_r denotes the relay transmission power. For a fair comparison, we assume that $P_1 = P_r = P_2 = P_s$.

3) IRS-OMA: IRS assisted cooperative OMA also includes two phases. During the i-th phase, the source serves U_i with the help of the IRS. Therefore, the outage probability experienced by U_1 is given by

$$\mathrm{P}_1^{\mathrm{I-OMA}} = \mathrm{P}\left(\frac{1}{2}\log\left(1+P_0\frac{\left|\mathbf{g}_1^H\mathbf{\Theta}\mathbf{g}_0\right|^2}{d_r^\alpha d_{r1}^\alpha}\right) < R_1\right), \quad (4)$$

where P_0 denotes the transmit power of s_1 in IRS-OMA. For a fair comparison, we assume that $P_0 = P_s$. The outage probability for U_2 can be obtained similarly.

III. Performance Analysis

It is straightforward to observe that U_2's outage performance in IRS-NOMA is much better than those of the benchmarking schemes. Because the analysis of U_2's outage probability is similar to the case without the IRS, in the remainder of the letter, we mainly focus on the outage probability experienced by U_1.

By assuming that the fading is Rayleigh distributed, it is straightforward to show that the outage probability achieved by conventional relaying is given by

$$\mathrm{P}_1^{\mathrm{OMA}} = \left(1-e^{-d_2^\alpha\left(2^{4R_1}-1\right)P_1^{-1}}\right) + e^{-d_2^\alpha\left(2^{4R_1}-1\right)P_1^{-1}} \times \left(1-e^{-d_{12}^\alpha\left(2^{4R_1}-1\right)P_1^{-1}}\right). \quad (5)$$

The evaluation of the outage probabilities, $\mathrm{P}_1^{\mathrm{NOMA}}$ and $\mathrm{P}_1^{\mathrm{I-OMA}}$, depends on how the phase shifting matrix $\mathbf{\Theta}$ is designed, where two designs with different tradeoffs between performance and complexity are introduced in the following.

A. Coherent Phase Shifting

Define $\mathbf{g}_i^H\mathbf{\Theta}\mathbf{g}_0$ as follows:

$$\xi_N \triangleq \mathbf{g}_i^H\mathbf{\Theta}\mathbf{g}_0 = \sum_{n=1}^{N} e^{-j\theta_n} g_{0,n}g_{i,n}, \quad (6)$$

where $g_{i,n}$ and $g_{0,n}$ denote the n-th elements of $\mathbf{g}_i$ and $\mathbf{g}_0$, respectively, and θ_n denotes the phase shift of the n-th reflecting element of the IRS.

Assume that the phase of $g_{0,n}g_{i,n}$ can be acquired by the source. For the coherent phase shifting design, the phase shifts of the IRS are matched with the phases of the IRS fading gains, which yields the following:

$$\xi_N = \sum_{n=1}^{N} \left|g_{0,n}g_{i,n}\right|. \quad (7)$$

The evaluation of the outage probabilities requires knowledge of the probability density function (pdf) of ξ_N, which is difficult to obtain. Therefore, two approximations are considered in the following subsections.

1) CLT-based Approximation: We note that the $|g_{0,n}g_{i,n}|$, $1 \le n \le N$, are independent and identically distributed (i.i.d.), and hence ξ_N is a sum of i.i.d. random variables, which motivates the use of the CLT.

As shown in [9], [10], the pdf of $|g_{0,n}g_{i,n}|^2$ is given by

$$f_{|g_{0,n}g_{i,n}|^2}(x) = 2K_0\left(2\sqrt{x}\right), \quad (8)$$

which can be used to find the pdf of $|g_{0,n}g_{i,n}|$ as follows:

$$f_{|g_{0,n}g_{i,n}|}(y) = 4yK_0\left(2y\right), \quad (9)$$

where $K_i(\cdot)$ denotes the modified Bessel function of the second kind.

The use of the CLT requires the mean and the variance of $|g_{0,n}g_{i,n}|$, which can be obtained as follows:

$$\mu_{|g_{0,n}g_{i,n}|} = \int_0^\infty 4y^2K_0\left(2y\right)dy = \frac{\pi}{4}, \quad (10)$$

and

$$\sigma^2_{|g_{0,n}g_{i,n}|} = \int_0^\infty 4y^3K_0\left(2y\right)dy - \frac{\pi^2}{16} = 1-\frac{\pi^2}{16}, \quad (11)$$

which follows from [11, (6.561.16)]. By using the CLT, ξ_N can be approximated as the following Gaussian random variable:

$$\sqrt{N}\left(\frac{\xi_N}{N} - \mu_{|g_{0,n}g_{i,n}|}\right) \sim \mathcal{N}\left(0, \sigma^2_{|g_{0,n}g_{i,n}|}\right). \quad (12)$$

Therefore, the outage probability of IRS-NOMA can be approximated as follows:

$$\mathrm{P}_1^{\mathrm{NOMA}} = \mathrm{P}\left(\mathbf{g}_1^H\mathbf{\Theta}\mathbf{g}_0 < \sqrt{\epsilon_1}\right) \approx \frac{1}{2} + \frac{1}{2}\phi\left(\frac{\sqrt{N}\left(\frac{\sqrt{\epsilon_1}}{N} - \mu_{|g_{0,n}g_{i,n}|}\right)}{\sqrt{2}\sigma_{|g_{0,n}g_{i,n}|}}\right), \quad (13)$$

where $\epsilon_1 = \frac{d_r^\alpha d_{r1}^\alpha \epsilon}{P_s(c_1^2 - \epsilon c_2^2)}$, $\epsilon = 2^{R_1}-1$, and $\phi(x) \triangleq \frac{2}{\sqrt{\pi}}\int_0^x e^{-t^2}dt$. It is assumed in this letter that $c_1^2 > \epsilon c_2^2$, otherwise $\mathrm{P}_1^{\mathrm{NOMA}} = 1$. The outage probability for IRS-OMA can be obtained similarly by replacing ϵ_1 with $\epsilon_2 = \frac{d_r^\alpha d_{r1}^\alpha\left(2^{2R_1}-1\right)}{P_0}$ in (13).

2) An upper bound: As shown in Section IV, the CLT-based approximation is not accurate in the high SNR regime, which motivates the development of a tight bound for the outage probability. To this end, we focus on IRS-NOMA. An upper bound on the outage probability is given in the following lemma.

Lemma 1. *Assume that N is an even number and denote $\bar{N} = \frac{N}{2}$. The outage probability achieved by IRS-NOMA is upper bounded as follows:*

$$\mathrm{P}_1^{\mathrm{NOMA}} \le \frac{2^N\pi^{\frac{N}{2}}\Gamma^N\left(\frac{3}{2}\right)}{(3\bar{N}-1)!}2^{-3\bar{N}}\gamma\left(3\bar{N}, 2\sqrt{\epsilon_1}\right), \quad (14)$$

where $\gamma(\cdot,\cdot)$ denotes the incomplete Gamma function and $\Gamma(\cdot)$ denotes the Gamma function.

Proof. See Appendix A. □

Remark: At high SNR, $\epsilon_1 \to 0$, which yields the following approximation for the upper bound shown in (14):

$$\mathrm{P}_1^{\mathrm{NOMA}} \leq 2^{N-3\bar{N}} \pi^{\frac{N}{2}} \Gamma^N \left(\frac{3}{2}\right) \frac{2^{3\bar{N}}}{(3\bar{N})!} \epsilon_1^{\frac{3}{4}N} \doteq \frac{1}{P_0^{\frac{3}{4}N}}, \quad (15)$$

where $\doteq$ denotes exponential equality [12]. Eq. (15) indicates that $\frac{3}{4}N$ is an achievable diversity order. It is important to point out that the full diversity gain, N, is also achievable, as shown in the following. By using the fact that $\xi_N \geq |g_{0,n} g_{i,n}|$, for $1 \leq n \leq N$, $\mathrm{P}_1^{\mathrm{NOMA}}$ can be upper bounded as follows:

$$\begin{aligned} \mathrm{P}_1^{\mathrm{NOMA}} &\leq \left(\int_0^{\epsilon_1} f_{|g_{0,n} g_{i,n}|^2}(x) dx \right)^N \quad (16) \\ &= \left(1 - 2\epsilon_1^{\frac{1}{2}} K_1\left(2\epsilon_1^{\frac{1}{2}}\right)\right)^N \approx \left(-\epsilon_1 \log \epsilon_1\right)^N \doteq \frac{1}{P_0^N}, \end{aligned}$$

which shows that the full diversity gain N is achievable. Although the upper bound in (16) is useful for the study of the diversity gain, we note that it is a bound much looser than the upper bound shown in Lemma 1, particularly for the case of large N. $\mathrm{P}_1^{\mathrm{I-OMA}}$ can be similarly obtained as $\mathrm{P}_1^{\mathrm{NOMA}}$.

B. Random Phase Shifting

The use of random phase shifting can avoid the requirement of perfect phase adjustment and reduce the system overhead needed for acquiring CSI at the source. Recall ξ_N as shown in (6), where θ_n is randomly chosen for random phase shifting.

Different from the coherent phase shifting case, ξ_N is a sum of complex-valued random variables, and the imaginary and real parts of $e^{-j\theta_n} g_{0,n} g_{i,n}$ are correlated, which means that the CLT is not directly applicable. In the following, we will show that ξ_N can be still approximated as a complex Gaussian random variable. We first note that, for small N, ξ_N is not complex Gaussian distributed, as can be seen from the following special case.

Proposition 1. *For the special case of $N = 1$, the pdf of the real and imaginary parts of ξ_N is given by*

$$f_{\mathrm{Re}\{\xi_1\}}(x) = e^{-2|x|}. \quad (17)$$

Proof. See Appendix B. □

However, by increasing N, the Gaussian approximation becomes applicable to ξ_N, as shown in the following lemma.

Lemma 2. *When $N \to \infty$, ξ_N can be approximated as a complex Gaussian random variable with zero mean and variance N, i.e.,*

$$\xi_N \to \mathcal{CN}(0, N). \quad (18)$$

Proof. See Appendix C. □

Therefore, the outage probabilities achieved by IRS with random phase shifting can be approximated as follows:

$$\mathrm{P}_1^{\mathrm{NOMA}} \approx 1 - e^{-\frac{\epsilon_1}{N}}, \quad \& \quad \mathrm{P}_1^{\mathrm{I-OMA}} \approx 1 - e^{-\frac{\epsilon_2}{N}}, \quad (19)$$

which indicates that IRS transmission with random phase shifting realizes a diversity order of one.

Phase shift selection: As shown in the next section, random phase shifting cannot effectively use the spatial degrees of freedom, although it can be implemented at low complexity. A better tradeoff between performance and complexity can be realized by carrying out phase shift selection, as described in the following. The IRS uses Q sets of random phase shifts to send Q pilot signals. U_1 informs the source which set of phase shifts it prefers. The use of this simple phase selection can significantly improve the performance of IRS transmission, as shown in the next section. We also note that the effective channel gains, ξ_N, obtained with different sets of random phases are not independent, which makes it difficult to develop analytical results for the proposed phase selection scheme.

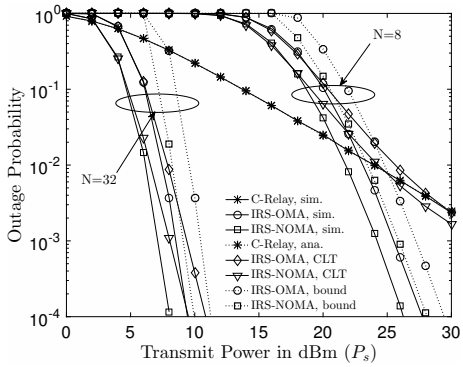

Fig. 1. IRS-OMA and IRS-NOMA with the coherent phase shifting scheme vs conventional relaying.

IV. Numerical Studies

In this section, the performance of the three considered transmission schemes is evaluated by computer simulations. Without loss of generality, we choose $c_1^2 = 0.8$, $c_2^2 = 0.2$, $d_2 = d_r = 20$ m, $d_{r1} = d_{12} = 10$ m, $\alpha = 4$, $R_1 = 1.8$ bit per channel use (BPCU). $P_1 = P_2 = P_r = P_s$. The noise power is -70 dBm. IRS-NOMA with coherent phase shifting is studied first in Fig. 1. As can be observed in the figure, conventional relaying can outperform the two IRS transmission schemes, particularly in the low SNR regime. This performance loss is due to the fact that IRS transmission suffers from severe path loss, $d_r^\alpha d_{r1}^\alpha$, as previously pointed out in [13]. However, by increasing the transmission power or the number of reflecting elements on the IRS, the IRS schemes eventually outperform conventional relaying, where the performance of IRS-NOMA is always better than that of IRS-OMA. The accuracy of the developed CLT approximation and the upper bound is also evaluated in the figure. As can be seen from the figure, in the low SNR regime, the CLT based approximation is accurate, and the developed upper bound is more accurate in the high SNR regime.

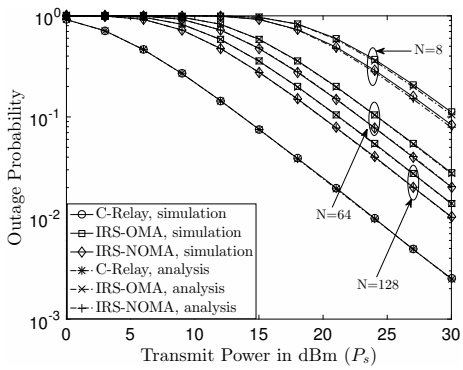

Fig. 2. The impact of random phase shifting on IRS transmission.

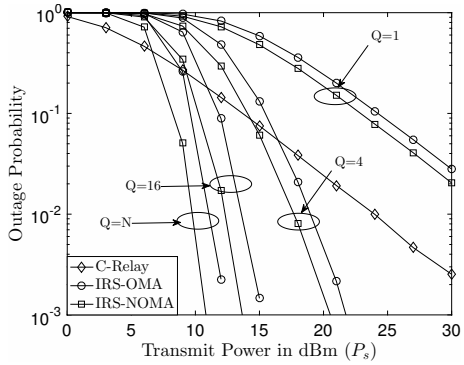

Fig. 3. Impact of phase shift selection on IRS transmission. $N = 64$

In Fig. 2, the impact of random phase shifting on IRS transmission is investigated. Recall that the motivation to use random phase shifting is that it can significantly reduce the system overhead and does not require complicated phase control mechanisms compared to coherent phase shifting. However, Fig. 2 shows that conventional relaying outperforms IRS transmission, although increasing N is helpful to reduce the performance gap. The reason for this performance loss is due to the fact that random phase shifting cannot efficiently utilize the spatial degrees of freedom offered by IRS. By implementing the proposed phase selection scheme, the performance of IRS transmission can be significantly improved. As shown in Fig. 3, with $Q = 4$, IRS-NOMA can realize a power reduction of 10 dBm at an outage probability of 10^{-3}, compared to conventional relaying. Figs. 2 and 3 also show that IRS-NOMA always outperforms IRS-OMA, which is consistent with Fig. 1. Furthermore, Fig. 2 demonstrates the accuracy of the approximation based on Lemma 2.

V. Conclusions

In this letter, the impact of two phase shifting designs on the performance of IRS-NOMA has been studied. Analytical results were developed to show that the two designs achieve different tradeoffs between system performance and complexity. Simulation results were provided to show the accuracy of the obtained analytical results and to compare IRS-NOMA to conventional relaying and IRS-OMA. For coherent phase shifting, the pdf of the effective channel gain, ξ_N, was evaluated in this letter by using two types of approximations, and finding an exact expression for the pdf is an important direction for future research.

Appendix A
Proof for Lemma 1

The outage probability achieved by IRS-OMA is given as follows:

$$\mathrm{P}_1^{\mathrm{I-OMA}} = \int\limits_{\sum_{i=1}^{N} y_i < \sqrt{\epsilon_1}} \cdots \int \prod_{i=1}^{N} f_{|g_{0,n}g_{i,n}|}(y_i) dy_i. \quad (20)$$

The fact that the pdf of $|g_{0,n}g_{i,n}|$, $f_{|g_{0,n}g_{i,n}|}(y_i)$, contains the Bessel function is the main reason why the performance analysis is difficult. We note that an upper bound on the Bessel function was provided in [14] as follows:

$$K_0(x) \leq \frac{\sqrt{\pi}e^{-x}}{\sqrt{2x}}. \quad (21)$$

By using this upper bound on the Bessel function, the pdf of $|g_{0,n}g_{i,n}|$ shown in (9) can be upper bounded as follows:

$$f_{|g_{0,n}g_{i,n}|}(y) \leq 4y\frac{\sqrt{\pi}e^{-2y}}{\sqrt{4y}} = 2\pi^{\frac{1}{2}}y^{\frac{1}{2}}e^{-2y} \triangleq g(y). \quad (22)$$

Because of the simple expression of $g(y)$, an upper bound on the pdf of the sum, $\sum_{i=1}^{N} y_i$, can be obtained, as shown in the following. First, the Laplace transform of the upper bound $g(y)$ can be obtained as follows:

$$\mathcal{L}\left(g(y)\right) = 2\pi^{\frac{1}{2}} \int_0^{\infty} e^{-sy} y^{\frac{1}{2}} e^{-2y} dy = \frac{2\pi^{\frac{1}{2}}\Gamma\left(\frac{3}{2}\right)}{(s+2)^{\frac{3}{2}}}. \quad (23)$$

By using the fact that y_i is i.i.d., the pdf of the sum, denoted by $f_{\sum_{i=1}^{N} y_i}(y)$, can be upper bounded as follows:

$$f_{\sum_{i=1}^{N} y_i}(y) \leq \mathcal{L}^{-1}\left(\frac{2^N \pi^{\frac{N}{2}} \Gamma^N\left(\frac{3}{2}\right)}{(s+2)^{\frac{3N}{2}}}\right). \quad (24)$$

Assume that N is an even number and let $\bar{N} = \frac{N}{2}$. An upper bound on the pdf of the sum can be obtained as follows:

$$f_{\sum_{i=1}^{N} y_i}(y) \leq \frac{2^N \pi^{\frac{N}{2}} \Gamma^N\left(\frac{3}{2}\right)}{(3\bar{N}-1)!} y^{3\bar{N}-1} e^{-2y}. \quad (25)$$

Therefore, the outage probability achieved by IRS-OMA can be upper bounded as follows:

$$\begin{aligned} \mathrm{P}_1^{\mathrm{I-OMA}} &\leq \int_0^{\sqrt{\epsilon_1}} \frac{2^N \pi^{\frac{N}{2}} \Gamma^N\left(\frac{3}{2}\right)}{(3\bar{N}-1)!} y^{3\bar{N}-1} e^{-2y} dy \quad (26) \\ &= \frac{2^N \pi^{\frac{N}{2}} \Gamma^N\left(\frac{3}{2}\right)}{(3\bar{N}-1)!} 2^{-3\bar{N}} \gamma\left(3\bar{N}, 2\sqrt{\epsilon_1}\right). \end{aligned}$$

Thus, the lemma is proved.

Appendix B
Proof for Proposition 1

Recall that $g_{0,n}$ and $g_{i,n}$ are complex Gaussian distributed with zero mean and unit variance, i.e., $g_{0,n} \sim \mathcal{CN}(0,1)$ and $g_{i,n} \sim \mathcal{CN}(0,1)$. Without loss of generality, denote $g_{0,n}$ and $g_{i,n}$ by $g_{0,n} = a_n + jb_n$ and $g_{i,n} = c_n + jd_n$, respectively, where a_n, b_n, c_n, and d_n are i.i.d., and follow $\mathcal{N}\left(0, \frac{1}{2}\right)$. Therefore, ξ_1 can be written as follows:

$$\begin{aligned} \xi_1 = &\left(a_n c_n - b_n d_n\right)\cos\theta_n - \left(a_n d_n + b_n c_n\right)\sin\theta_n \quad (27) \\ &+ j\left(\left(a_n c_n - b_n d_n\right)\sin\theta_n + \left(a_n d_n + b_n c_n\right)\cos\theta_n\right). \end{aligned}$$

We note that the real and imaginary parts of ξ_1 are identically distributed, and hence in the following, we focus on the real part of ξ_1 which can be further written as follows:

$$\mathrm{Re}\{\xi_1\} = a_n \tilde{c}_n - b_n \tilde{d}_n, \quad (28)$$

where $\tilde{c}_n$ and $\tilde{d}_n$ are defined as follows:

$$\begin{bmatrix} \tilde{c}_n \\ \tilde{d}_n \end{bmatrix} = \begin{bmatrix} \cos\theta_n & -\sin\theta_n \\ \sin\theta_n & \cos\theta_n \end{bmatrix} \begin{bmatrix} c_n \\ d_n \end{bmatrix}. \quad (29)$$

We further note that the transformation matrix in (29) is a unitary matrix, and c_n and d_n are i.i.d. Gaussian random variables. Therefore, $\tilde{c}_n, \tilde{d}_n \sim \mathcal{N}\left(0, \frac{1}{2}\right)$ since a unitary transformation does not change the statistical property of Gaussian variables.

Therefore, the cumulative distribution function (CDF) of $\mathrm{Re}\{\xi_1\}$ is given by

$$\begin{aligned}\mathrm{P}(\mathrm{Re}\{\xi_1\}<\mathrm{y}) =&\mathrm{P}(a_n\tilde{c}_n - b_n\tilde{d}_n < y) \\ \overset{(i)}{=}&E_{\tilde{c}_n,\tilde{d}_n}\left\{\int_{-\infty}^{y}\frac{1}{\sqrt{\pi(\tilde{c}_n^2+\tilde{d}_n^2)}}e^{-\frac{x^2}{\tilde{c}_n^2+\tilde{d}_n^2}}dx\right\} \\ \overset{(ii)}{=}&\int_0^{\infty}\int_{-\infty}^{y}\frac{1}{\sqrt{\pi z}}e^{-\frac{x^2}{z}}dx e^{-z}dz,\end{aligned} \tag{30}$$

where step (i) follows the fact that $a_n\tilde{c}_n - b_n\tilde{d}_n$ is a sum of two i.i.d. Gaussian variables, a_n and b_n, by treating $\tilde{c}_n$ and $-\tilde{d}_n$ as the weighting constants, and step (ii) follows by the fact that $z \triangleq \tilde{c}_n^2 + \tilde{d}_n^2$ is exponentially distributed.

The CDF of $\mathrm{Re}\{\xi_1\}$ can be simplified as follows:

$$\begin{aligned}\mathrm{P}(\mathrm{Re}\{\xi_1\}<\mathrm{y}) =&\int_{-\infty}^{y}\frac{1}{\sqrt{\pi}}\int_0^{\infty}z^{-\frac{1}{2}}e^{-\frac{x^2}{z}-z}dzdx \\ \overset{(iii)}{=}&\int_{-\infty}^{y}e^{-2|x|}dx,\end{aligned} \tag{31}$$

where step (iii) follows [11, (3.471.15)]. By finding the derivative of the CDF, the pdf in the proposition can be obtained and the proof is complete.

Appendix C
Proof for Lemma 2

The lemma can be proved by two steps as shown in the following two subsections.

A. $\mathrm{Re}\{\xi_N\}$, $\mathrm{Im}\{\xi_N\} \sim \mathcal{N}\left(0, \frac{N}{2}\right)$ *for* $N \to \infty$

Since $\mathrm{Re}\{\xi_N\}$ and $\mathrm{Im}\{\xi_N\}$ are identically distributed, we will focus on $\mathrm{Re}\{\xi_N\}$, without loss of generality. Recall that $\mathrm{Re}\{\xi_N\} = \sum_{n=1}^{N}\mathrm{Re}\{e^{-j\theta_n}g_{0,n}g_{i,n}\}$.

Without directly using the CLT, the approximation for the pdf of $\mathrm{Re}\{\xi_N\}$ can be straightforwardly obtained as follows. By applying Proposition 1, the characteristic function of the pdf of $\mathrm{Re}\{e^{-j\theta_n}g_{0,n}g_{i,n}\}$ can be obtained as follows:

$$\psi_{\mathrm{Re}\{e^{-j\theta_n}g_{0,n}g_{i,n}\}}(t) = \int_{-\infty}^{\infty}e^{itx}f_{\xi_1}(x)dx = \frac{4}{4+t^2}. \tag{32}$$

By using the fact that $\mathrm{Re}\{e^{-j\theta_n}g_{0,n}g_{i,n}\}$ is independent from $\mathrm{Re}\{e^{-j\theta_m}g_{0,m}g_{i,m}\}$ for $n \neq m$, the characteristic function of the pdf of $\mathrm{Re}\{\xi_N\}$ can be obtained as follows:

$$\psi_{\mathrm{Re}\{\xi_N\}}(t) = \frac{4^N}{(4+t^2)^N} \underset{N\to\infty}{\to} e^{-\frac{Nt^2}{4}}, \tag{33}$$

where the approximation follows by applying the limit of the exponential function. Therefore, $\mathrm{Re}\{\xi_N\}$ can be approximated as a Gaussian random variable since $e^{-\frac{Nt^2}{4}}$ is the characteristic function of a Gaussian random variable.

B. $\mathrm{Re}\{\xi_N\}$ *and* $\mathrm{Im}\{\xi_N\}$ *are Independent for* $N \to \infty$

We have proved that $\mathrm{Re}\{\xi_N\}, \mathrm{Im}\{\xi_N\} \sim \mathcal{N}\left(0, \frac{N}{2}\right)$, for $N \to \infty$. Therefore, the independence between the two random variables can be proved by showing them to be jointly Gaussian distributed and also uncorrelated.

In order to show that $\mathrm{Re}\{\xi_N\}$ and $\mathrm{Im}\{\xi_N\}$ are jointly Gaussian distributed, we first build an arbitrary linear combination of $\mathrm{Re}\{\xi_N\}$ and $\mathrm{Im}\{\xi_N\}$ with β_1 and β_2 as follows:

$$\begin{aligned}&\beta_1\mathrm{Re}\{\xi_N\} + \beta_2\mathrm{Im}\{\xi_N\} \\ =&\sum_{n=1}^{N}a_n(\beta_1\tilde{c}_n + \beta_2\tilde{d}_n) - b_n(\beta_1\tilde{d}_n - \beta_2\tilde{c}_n).\end{aligned} \tag{34}$$

Note that $(\beta_1\tilde{c}_n + \beta_2\tilde{d}_n)$ and $(\beta_1\tilde{d}_n - \beta_2\tilde{c}_n)$ are independent and identically Gaussian distributed since they are constructed from $\tilde{c}_n$ and $\tilde{d}_n$ with two orthogonal coefficient vectors $\begin{bmatrix}\beta_1 & \beta_2\end{bmatrix}^T$ and $\begin{bmatrix}-\beta_2 & \beta_1\end{bmatrix}^T$. By following the steps in the previous subsection, it is straightforward to show that the linear combination is also Gaussian distributed, which means that $\mathrm{Re}\{\xi_\mathrm{N}\}$ and $\mathrm{Im}\{\xi_\mathrm{N}\}$ are jointly Gaussian distributed.

The correlation between $\mathrm{Re}\{\xi_N\}$ and $\mathrm{Im}\{\xi_N\}$ is given by

$$\begin{aligned}&\mathcal{E}\left\{\mathrm{Re}\{\mathbf{g}_i^H\mathbf{\Theta}_p\mathbf{g}_0\}\mathrm{Im}\{\mathbf{g}_i^H\mathbf{\Theta}_p\mathbf{g}_0\}\right\} \\ =&\mathcal{E}\left\{\left(\sum_{n=1}^{N}a_n\tilde{c}_n - b_n\tilde{d}_n\right)\left(\sum_{n=1}^{N}a_n\tilde{d}_n + b_n\tilde{c}_n\right)\right\} = 0,\end{aligned} \tag{35}$$

which follows the fact that a_n, b_n, $\tilde{c}_n$ and $\tilde{d}_n$ are i.i.d. with zero mean, where $\mathcal{E}\{\cdot\}$ denotes the expectation. Therefore, the independence between $\mathrm{Re}\{\xi_N\}$ and $\mathrm{Im}\{\xi_N\}$ is proved.

References

[1] Q. Wu and R. Zhang, "Intelligent reflecting surface enhanced wireless network via joint active and passive beamforming," *IEEE Trans. Wireless Commun.*, vol. 18, no. 11, pp. 5394–5409, Nov. 2019.

[2] M. D. Renzo, M. Debbah, D.-T. Phan-Huy, A. Zappone, M.-S. Alouini, C. Yuen, V. Sciancalepore, G. C. Alexandropoulos, J. Hoydis, H. Gacanin, J. de Rosny, A. Bounceu, G. Lerosey, and M. Fink, "Smart radio environments empowered by AI reconfigurable meta-surfaces: An idea whose time has come," Available on-line at arXiv:1903.08925.

[3] Q. Wu and R. Zhang, "Towards smart and reconfigurable environment: Intelligent reflecting surface aided wireless network," *IEEE Commun. Mag.*, (to appear in 2020).

[4] V. Jamali, A. M. Tulino, G. Fischer, R. Mller, and R. Schober, "Intelligent reflecting and transmitting surface aided millimeter wave massive MIMO," Available on-line at arXiv:1902.07670.

[5] Z. Ding, L. Dai, R. Schober, and H. V. Poor, "NOMA meets finite resolution analog beamforming in massive MIMO and millimeter-wave networks," *IEEE Commun. Lett.*, vol. 21, no. 8, pp. 1879–1882, Aug. 2017.

[6] Q. Zhang, W. Saad, and M. Bennis, "Reflections in the sky: Millimeter wave communication with UAV-carried intelligent reflectors," in *Proc. IEEE Global Commun. Conf. (GLOBECOM)*, Hawaii, US, Dec. 2019.

[7] B. Lyu, D. T. Hoang, S. Gong, D. Niyato, and D. I. Kim, "IRS-based wireless jamming attacks: When jammers can attack without power," Available on-line at arXiv:2001.01887.

[8] C. Pan, H. Ren, K. Wang, M. Elkashlan, A. Nallanathan, J. Wang, and L. Hanzo, "Intelligent reflecting surface aided MIMO broadcasting for simultaneous wireless information and power transfer," Available on-line at arXiv:1908.04863.

[9] Z. Ding and H. V. Poor, "A simple design of IRS-NOMA transmission," *IEEE Commun. Lett.*, Available on-line at arXiv:1907.09918.

[10] N. C. Sagias, "On the ASEP of decode-and-forward dual-hop networks with pilot-symbol assisted M-PSK," *IEEE Trans. Commun.*, vol. 62, no. 2, pp. 510–521, Feb. 2014.

[11] I. S. Gradshteyn and I. M. Ryzhik, *Table of Integrals, Series and Products*, 6th ed. New York: Academic Press, 2000.

[12] L. Zheng and D. N. C. Tse, "Diversity and multiplexing : A fundamental tradeoff in multiple antenna channels," *IEEE Trans. Inform. Theory*, vol. 49, pp. 1073–1096, May 2003.

[13] E. Björnson, O. Özdogan, and E. G. Larsson, "Intelligent reflecting surface vs. decode-and-forward: How large surfaces are needed to beat relaying?" Available on-line at arXiv:1906.03949.

[14] Z.-H. Yang and Y.-M. Chu, "On approximating the modified bessel function of the second kind," *Journal of Inequalities and Applications*, vol. 41, Dec. 2017.